CHEMELECTROCHEM
COMMUNICATIONS

ChemPubSoc Europe

DOI: 10.1002/celc.201300140

Oxygen Reduction at Soft Interfaces Catalyzed by In Situ-Generated Reduced Graphene Oxide

Shokoufeh Rastgar,[a, b] Haiqiang Deng,[a] Fernando Cortés-Salazar,[a] Micheál D. Scanlon,[a] Medeya Pribil,[c] Véronique Amstutz,[a] Arkady A. Karyakin,[c] Saeed Shahrokhian,[b] and Hubert H. Girault*[a]

Graphene oxide (GO) in water was reduced heterogeneously by decamethylferrocene (DMFc) or ferrocene (Fc) in 1,2-dichloroethane (DCE), which could then act as a catalyst for an interfacial oxygen reduction reaction (ORR) and production of hydrogen peroxide (H_2O_2). The reduced graphene oxide (RGO) produced at the liquid/liquid interface was characterized by using electron microscopy, spectroscopy (Raman, infrared, and electron energy loss), and electrochemical techniques.

The oxygenated functional groups at the edge/defects of the RGO surface activate O_2 adsorption, forming superoxide-like adducts that can be protonated at the liquid/liquid interface and reduced by DMFc or Fc. This process is facilitated by the higher electrical conductivity of the RGO sheets. The key feature of this catalytic reaction is the in situ partial-reduction of GO at the liquid/liquid interface, forming an efficient and inexpensive catalyst for the production of H_2O_2.

Electrochemistry at polarized interfaces between two immiscible electrolyte solutions (ITIES) has developed over the past 30 years, in which charge-transfer (electron- and ion-transfer) reactions have found applications in areas such as phase-transfer catalysis, solvent-extraction processes, chemical sensing, solar-energy-conversion systems, drug release and delivery, and in mimicking the function of biological membranes.[1] Liquid/liquid interfaces provide a unique platform at which to study ORRs, at which aqueous protons react with organic solubilized electron donors in the absence or presence of adsorbed catalysts, usually through a proton-coupled electron-transfer (PCET) reaction.[2] The molecular catalysts studied include cobalt,[3] free-base porphyrins,[4] and in situ-deposited platinum particles.[5] The ORR proceeds either by a $4e^-/4H^+$ pathway to produce water or a $2e^-/2H^+$ route to yield H_2O_2, which is considered a green oxidant.

H_2O_2 is widely used in many industrial areas, particularly in the chemical industry or for environmental protection, and is currently produced on an industrial scale through the biphasic anthrahydroquinone oxidation (AO) process (representing ca. 95% of the world's H_2O_2 production).[6] Generally, anthrahydroquinone is oxidized by O_2 to produce H_2O_2 and anthraquinone and, subsequently, the formed anthraquinone is reduced back to the anthrahydroquinone by using H_2 in the presence of a metal catalyst. Both reactions occur in the organic phase, and H_2O_2 is recovered by extraction to the aqueous phase.[6] The advantage of the AO process is the very high yield of H_2O_2 generated per cycle. Conversely, side reactions generating organic byproducts need to be dealt with by regenerating the solution and by using separation techniques to eliminate such impurities. Conceptually, following the AO process, the reduction of O_2 was investigated at quinone-modified carbon surfaces. O_2 reduction to H_2O_2 was mediated by surface-bound quinone groups via superoxide anion intermediates,[7] and such modified electrodes have shown great catalytic activity towards the $2e^-/2H^+$ ORR. Recently, Fukuzumi et al. reviewed the current state-of-the-art process for the homogeneous and heterogeneous electrocatalytic production of H_2O_2 with a variety of metal complexes, including cobalt porphyrins, biscobalt porphyrin–corrole complexes, cytochrome c oxidase models, and Cu complexes, as ORR catalysts.[8] An important development is the production of H_2O_2 through the electrocatalytic $2e^-$ reduction of O_2, which is electrically powered by an integrated photovoltaic solar cell. Stored H_2O_2 can then be used as a sustainable solar fuel to generate power as H_2O_2 fuel cells.[8] Thus, implementing new efficient and inexpensive catalysts for the biphasic production of H_2O_2 is of high relevance and might lay the foundations for new industrial processes.

Graphene is a one-atom-thick planar sheet of sp^2-bonded carbon atoms densely arranged into a 2D honeycomb crystal lattice.[9] Thanks to the high specific surface area (theoretically 2630 $m^2 g^{-1}$ for single-layered graphene),[10] the large number of edge-planes/defects,[11] a high electron-transfer rate (15000 $cm^2 V^{-1} s^{-1}$), strong mechanical strength, and both excellent thermal and electrical conductivities,[12] graphene sheets are of interest in electrochemistry. GO, a precursor for graphene synthesis, consists of a hexagonal ring-based carbon network, having both (largely) sp^2-hybridized carbon atoms and (partly) sp^3-hybridized carbons. These carbon atoms bear oxygen-based functional groups in the form of hydroxyl and

[a] Dr. S. Rastgar, H. Deng, Dr. F. Cortés-Salazar, Dr. M. D. Scanlon, V. Amstutz, Prof. H. H. Girault
Laboratoire d'Electrochimie Physique et Analytique
Ecole Polytechnique Fédérale de Lausanne (EPFL)
Station 6, CH-1015, Lausanne (Switzerland)
Tel.: (+41) 21-693-3145
Fax: (+41) 21-693-3667
E-mail: hubert.girault@epfl.ch

[b] Dr. S. Rastgar, Prof. S. Shahrokhian
Department of Chemistry, Sharif University of Technology
Tehran 11155-9516 (Iran)

[c] M. Pribil, Prof. A. A. Karyakin
Chemistry and Material Science Faculties of M.V. Lomonosov
Moscow State University, 119991, Moscow (Russia)

Supporting Information for this article is available on the WWW under http://dx.doi.org/10.1002/celc.201300140.

epoxy moieties on the basal plane, with smaller amounts of carboxyl, carbonyl, phenol, lactone, and quinone groups at the sheet edges. These can be viewed as oxidized regions, disrupting the extended sp^2-conjugated network of the original honeycomb lattice-structured graphene sheet.[13] RGO, the more conductive product of the partial reduction of GO, has also been studied in recent years as a catalyst for the ORR, in both alkaline and acidic media, and has been considered for potential applications in microbial fuel cells.[14] Recently, it has been shown that GO and ferrocene composites can be prepared and employed for photoinduced charge-transfer processes.[15]

With the aim of developing an alternative biphasic system for H_2O_2 production, we investigated the catalytic properties of RGO towards O_2 reduction at the ITIES. RGO was generated in situ at the water/DCE interface by partial reduction of water-soluble GO with DMFc or Fc solubilized in the DCE phase. DMFc and Fc have dual roles, acting as electron donors for the reduction of GO adsorbed at the interface and, subsequently, as reductants for O_2 molecules adsorbed on the RGO sheets. RGO produced in this manner was characterized by using electron microscopy, spectroscopy [infrared (IR), electron-energy-loss (EELS) and Raman], in addition to electrochemical methods (see SI-1 and SI-2 in the Supporting Information for the preparation and characterization of RGO).

Cyclic voltammograms (CVs) were obtained at the water/DCE interface under aerobic conditions (Figure 1), unless stated otherwise, by using the four-electrode electrochemical

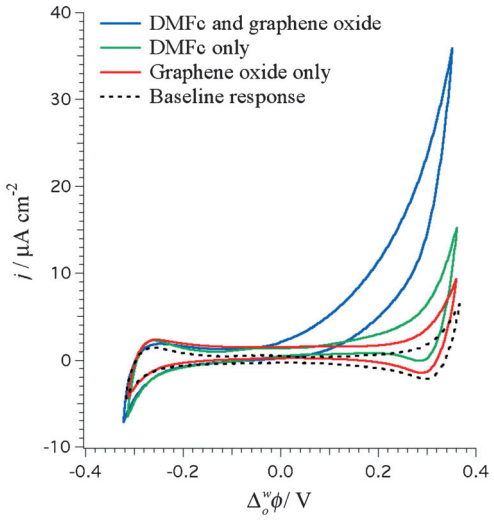

Figure 1. Cyclic voltammograms obtained under aerobic conditions, using the electrochemical cell outlined in Scheme 1 A, in the absence of both DMFc and GO (----- $x=0$, $y=0$, $z=100$), with only GO (—— $x=0$, $y=0.2$, $z=100$), with only DMFc (—— $x=1$, $y=0$, $z=100$) and with both DMFc and GO (—— $x=1$, $y=0.2$, $z=100$) present. Scan rate used: 50 mV s^{-1}.

cell outlined in Scheme 1 A. The baseline CV response of the background electrolytes, that is, protons (H^+) and chloride ions (Cl^-) in the acidic aqueous phase (*w*) and bis(triphenylphosphoranylidene) ammonium tetrakis(penta-fluorophenyl) borate (BATB) in DCE (*o*), exhibits a potential window that is limited by the transfer of H^+ and Cl^- from the aqueous phase

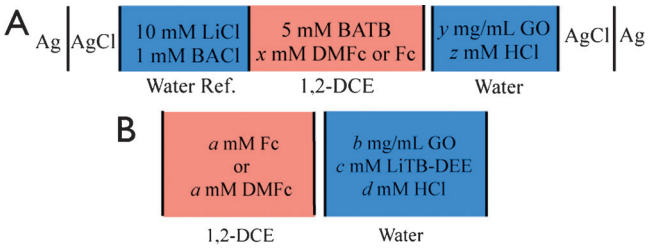

Scheme 1. A) Potentiostatic polarization and B) chemical polarization of the interface, showing compositions of the electrochemical cells used for ion-transfer voltammetry and the shake-flask experiments. All experiments, unless noted otherwise, were performed under aerobic conditions.

to the organic phase and vice-versa at the positive and negative potential limits, respectively. Upon introduction of 1 mM DMFc to the DCE phase, a current wave at positive potentials is observed, indicating an interfacial protonation of DMFc, which is associated with the production of H_2O_2, in agreement with previous reports.[3a,16] The subsequent addition of 0.2 mg mL^{-1} of GO to the aqueous phase leads to a considerable increase in this current, as well as a decrease in the onset potential of the current wave. The current may be further enhanced by dispersing higher concentrations of GO in the aqueous phase (see Figure SI-3.1 A in the Supporting Information). These results demonstrate the catalytic role of interfacial GO for O_2 reduction with DMFc in this biphasic system. Control experiments confirmed that these trends were only observed under aerobic conditions (see Figure SI-3.1 B in the Supporting Information). Moreover, a shift of the current-wave onset potential by approximately 60 mV pH^{-1} corroborated the role of the proton in this voltammetric signal (see Figure SI-3.1 C in the Supporting Information).

These observations unambiguously show that GO, O_2, H^+, and DMFc must all be present for the PCET-mediated ORR catalytic process to proceed, as outlined in Equation (1):

$$2\,DMFc + O_2 + 2\,H^+ \xrightarrow[\text{RGO catalyst}]{\text{in situ generated}} 2\,DMFc^+ + H_2O_2 \qquad (1)$$

Crucially, the enhanced conductivity of in situ-formed RGO (relative to GO) facilitates electron injection by DMFc to the catalytically active ORR sites. The current wave at positive potentials varies linearly with the square root of the scan rate (data not shown), indicating that this process is limited by the diffusion of DMFc to the interface, as all other species are in excess.

On replacing DMFc (standard redox potential in DCE versus the aqueous standard hydrogen electrode (SHE), $[E^0_{DMFc^+/DMFc}]^o_{SHE} = 0.04$ V)[17] with a weaker reductant such as Fc ($[E^0_{Fc^+/Fc}]^o_{SHE} = 0.64$ V),[2] the current wave associated with the PCET process is no longer evident, as it is shifted in a positive direction, that is, outside of the available potential window, because of the difference between the redox potentials of DMFc and Fc. Nonetheless, an enhanced production of ferrocenium ions (Fc^+) in the presence of GO was clearly observed by ion-transfer voltammetry (see Figure SI-3.1 D in the Supporting Information), indicating that an electron transfer event involving Fc occurs at the edge of the potential window (i.e. the reduc-

tion of GO to RGO and, as shown vide infra, the subsequent PCET process).

The catalytic reduction of O_2 at RGO sheets was also investigated by shake-flask experiments, in which the polarization of the water/DCE interface was controlled chemically by distribution of a highly hydrophobic anion (TB^-), as described in Scheme 1 B and in the Experimental Section (see SI-1 in the Supporting Information). Under such conditions, the water/DCE interface is polarized positively,[18] and TB^- acts as a pump to drive H^+ from the aqueous phase to the DCE phase, forming the organic acid HTB. Evidence of the enhancement in rate of the oxidation of the electron donors by GO is clearly seen by comparing the UV/Vis spectra of the organic products [either decamethylferrocenium ($DMFc^+$) or Fc^+ ions, pre- and post-shake-flask, with and without GO present] and noting the increased production of the biphasic reaction ($\lambda_{max}=779$ and 620 nm, respectively) in the presence of GO (see Figure SI-4.1 in the Supporting Information). The data obtained in the absence of GO is in perfect agreement with that previously reported.[16b]

Quantitative real-time monitoring of $DMFc^+$ and Fc^+ was possible by following changes in their particular UV/Vis spectra with time at 779 and 620 nm, respectively (Figure 2). The resultant kinetically limited time profiles of the formation of $DMFc^+$

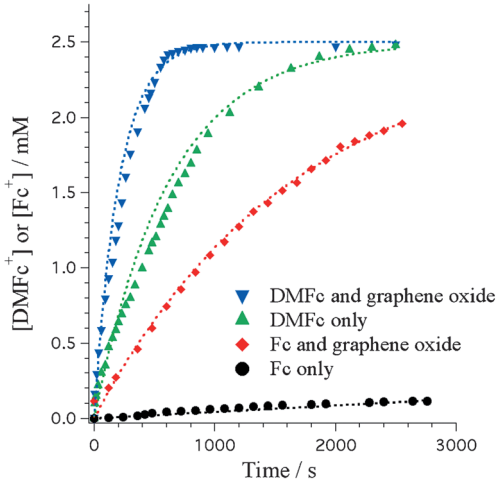

Figure 2. Kinetics of the biphasic oxidation of the electron donors in the absence and presence of GO. Monitoring the formation of $DMFc^+$ and Fc^+ through chemically controlled polarization (see Scheme 1 B) in the absence or presence of GO ($a=2.5$, $b=0$ or 0.2, $c=10$, $d=100$), as followed by recording changes in the UV/Vis absorbance at $\lambda_{max}=779$ and 620 nm, respectively, under aerobic conditions.

or Fc^+ in the absence and presence of GO show that the oxidation of the electron donors proceeds much faster in the presence of GO in water. Indeed, the apparent rate constants for each shake-flask experiment were calculated (see SI-5 in the Supporting Information) and found to be first order with respect to DMFc or Fc.[19] Increases in the rate of approximately 3.75 and 30 times were observed for GO with DMFc and Fc, respectively (Table 1). When GO is present, the increase in rate can be attributed to the oxidation of the electron donor when

Table 1. Apparent rate constants (k/s^{-1}) for the biphasic reaction and the corresponding catalyst-enhancement factor ($k/k_{no\ cat}$).

Electron donor/catalyst	k/s^{-1}	$k/k_{no\ catalyst}$
DMFc only	0.0016	1
DMFc and GO	0.0060	3.75
Fc only	0.00002	1
Fc and GO	0.0006	30

electrons are consumed to convert GO to RGO at the interface as well as to the subsequent RGO-catalyzed ORR reaction. The precise contribution of each process to the apparent rate was not deconvoluted during this study.

Finally, quantitative increases in concentration of the other biphasic reaction product, H_2O_2, in the aqueous post-shake-flask reaction for both electron donors in the presence and absence of GO were confirmed through a NaI titration, in which H_2O_2 oxidizes I^- to I^{3-}, see Figure 3, Table 2, and SI-6 in the Supporting Information. This is a crucial finding with respect to

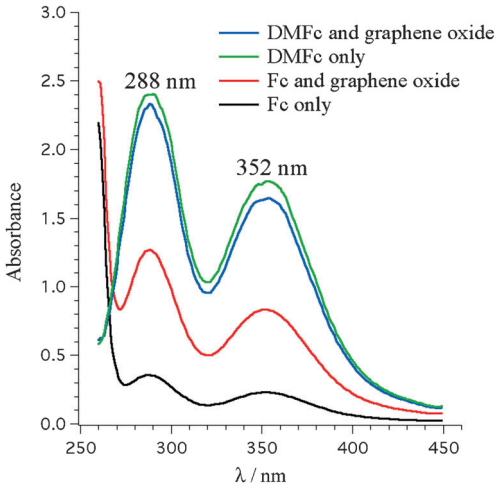

Figure 3. Monitoring the formation of H_2O_2. UV/Vis adsorption spectra of the aqueous phase after shake-flask reactions upon treatment with excess NaI for cells containing DMFc (the aqueous phase was diluted 10-fold prior to analysis) or Fc (aqueous phase undiluted), under aerobic conditions, either with or without GO ($a=2.5$, $b=0$ or 0.2, $c=10$, $d=100$, see Scheme 1 B). The reaction time for all experiments was 1 h.

the use of Fc as a reductant, as the increased quantity of H_2O_2 found in the presence of GO shows that Fc not only reduces GO but also that it is categorically involved in the PCET step in the ORR. Under biphasic aerobic conditions, DMFc is fully converted to $DMFc^+$ after 1 h, both in the presence and absence of GO. As a result, the quantities of H_2O_2 produced after 1 h in the presence or absence of GO for DMFc were identical within experimental error (±5% H_2O_2 yield), see Table 2. However, Fc is substantially converted to Fc^+ after 1 h in the presence of GO (88.4%), but significantly less so in its absence (6.96%). The more rapid conversion of Fc in the presence of GO suggests a considerable portion of the electrons donated by Fc are consumed to reduce GO to RGO. The remaining electrons are subsequently used in the RGO catalyzed reduction of O_2 with Fc,

Table 2. Detected H_2O_2 after shake-flask reaction for cells containing DMFc or Fc, under aerobic conditions, either with or without GO ($a=2.5$, $b=0$ or 0.2, $c=10$, $d=100$, see Scheme 1 B). H_2O_2 was detected through a NaI titration (see Figure 3 and the Supporting Information SI-6). Reaction time for all experiments was 1 h.

Electron donor/ catalyst	Detected H_2O_2 [mM]	Conversion[a] [%]	H_2O_2 per oxidized donor yield[b,c] [%]
DMFc and GO	0.535	100	42.80
DMFc only	0.576	100	46.08
Fc and GO	0.026	88.4	2.35
Fc only	0.0064	6.96	7.36

[a] The conversion represents the ratio of $DMFc^+$ (or Fc^+) detected by UV/Vis spectroscopy (after 1 h of shake-flask reaction) to the initial concentration of DMFc (or Fc). [b] The yield of H_2O_2 represents the ratio of the detected concentration of H_2O_2 (from NaI titration) to the theoretical H_2O_2 concentration, which is calculated stoichiometrically from the concentration of $DMFc^+$ (or Fc^+) after 1 h of reaction. [c] The results were verified by using two alternative methods to determine H_2O_2 concentrations in the aqueous phase, namely a Prussian Blue (PB) sensor[20] and a titanium-oxalate methodology[21] (data not shown). A very good agreement was found among all strategies employed.

and the catalysis effect is reflected in the larger concentration of H_2O_2 detected with Fc in the presence of GO after 1 h. The relatively low yields of H_2O_2 (calculated as discussed in Table 2) were expected, and are primarily a consequence of a portion of the available electrons being consumed to produce RGO in situ. It should be noted that the partial decomposition of H_2O_2 by the action of transition-metal compounds, such as DMFc and Fc, prior to detection with the NaI method, may also lower the yield.[6a] Thus, an inference may be made that, despite a portion of the electrons being consumed during the reaction to generate RGO in situ, the remaining electrons are utilized more efficiently during the RGO-catalyzed ORR (the mechanism of which is discussed below), thereby generating higher concentrations of H_2O_2 in shorter times in the presence of either electron donor.

The results herein clearly show that RGO prepared in situ at the liquid/liquid interface is a catalyst for the ORR. Indeed, the catalytic behavior of RGO for O_2 reduction at solid electrodes has been reported previously.[14,22] A key feature is that O_2 reduction stops at the peroxide stage, enabling its use as a catalyst for the synthesis of H_2O_2. This catalytic activity can be attributed to surface-bound oxygen-containing groups remaining at defect sites on the RGO sheets after reduction, as revealed by spectroscopic and electrochemical experiments. It is expected that the reduction of O_2 proceeds via a $2e^-/2H^+$ mechanism to yield H_2O_2, in which the quinone-type groups at the surface of the RGO sheets (RGO-Q) are initially chemically reduced to semiquinone radicals (RGO-$Q^{\bullet-}$) by an electron donor, such as DMFc or Fc in our case. Advantageously, DMFc and Fc are capable of injecting their electrons anywhere on the RGO backbone, thereby greatly increasing the cross-section of reaction between the electron donor and catalytic substrate. The rate-determining step (RDS) is expected to be the reaction between the chemically generated semiquinone radicals, adsorbed protons, and O_2, resulting in the formation of a protonated intermediate superoxo species (RGO-Q-$HO_2^{\bullet}$). Proton adsorption is critical to increase the reduction rate by accelerating the protonation of O_2. Further reduction by DMFc or Fc, and simultaneous reaction with an additional adsorbed proton, enables the release of H_2O_2 and the regeneration of the quinone-type groups at the surface of RGO [see Eqs. (2)–(4)]. This mechanism of quinone-mediated reduction of molecular O_2 to H_2O_2 is consistent with previous reports for O_2 reduction at quinone-modified electrode surfaces.[5,23]

$$RGO-Q+e^- \rightarrow RGO-Q^{\bullet-} \quad (2)$$

$$RGO-Q^{\bullet-}+O_2+H^+ \rightarrow RGO-Q\text{-}HO_2^{\bullet} \quad (3)$$

$$RGO-Q-HO_2^{\bullet}+e^-+H^+ \rightarrow RGO-Q+H_2O_2 \quad (4)$$

in which the electrons (e^-) are injected by DMFc or Fc.

In summary, a new approach for the two-phase reduction of O_2 has been developed by partially reducing GO at the ITIES. The resulting RGO is an efficient catalyst for the ORR because of quinone-type catalysis through the formation of a superoxo intermediate. The catalytic activity of RGO has been verified in this work by using two different reducing species, namely DMFc and Fc, of different electron-donating ability. The biphasic features of the employed strategy favor the collection of H_2O_2 by immediate extraction to the water phase and, thus, preventing further side reactions with organic solubilized Fc-derivatives or degradation in the DCE phase. In general, RGO can be considered for a biphasic H_2O_2 batch-production scheme where, upon completion of the cycle described above, the oxidized donor, that is, $DMFc^+$ or Fc^+, is recycled electrochemically in the same biphasic system after extraction of the solid RGO phase (see Figure 4). A two-step process is envisioned, in which the oxidized lipophilic electron donor is reduced at a cathode and the O_2 and protons are produced at the anode after replacement of the H_2O_2 solution with a fresh aqueous solution. In such biphasic electrolysis, the reduction of the oxidized donor is accompanied by a transfer of aqueous protons from the aqueous to the organic phase to regenerate the organic acid, HTB.

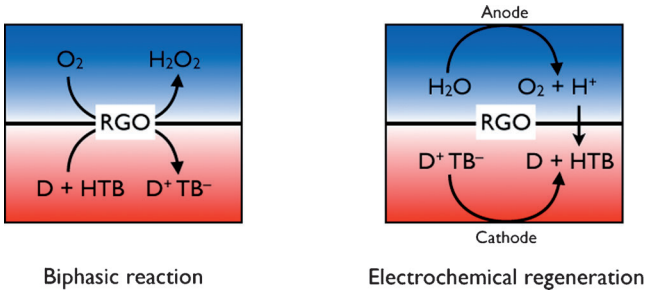

Figure 4. Possible batch production of H_2O_2 based on a RGO liquid/liquid interface system, in ehich D is an electron-donating species, such as DMFc or Fc.

Experimental Section

For experimental details, please see the Supporting Information.

Acknowledgements

S.R. and H.D. thank the Ministry of Science, Research, and Technology of Iran and the China Scholarship Council (CSC), respectively, for financial support. We are especially grateful to Dr. A. Duncan from CIME-EPFL for TEM, HRTEM, and EELS analyses of GO and RGO; F. Matteini from LMSC-EPFL and R. Gaal from EPSL-EPFL for Raman analyses of GO and RGO; A. Gasperini from LIMNO-EPFL for AFM analysis of GO films on glass; and D. Momotenko from LEPA-EPFL for fitting SECM data for quantification of GO and RGO's conductivities.

Keywords: electrochemistry · electron microscopy · graphene · H_2O_2 production · liquid/liquid interface

[1] Y. Shao in *Handbook of Electrochemistry* (Ed.: C. G. Zoski), Elsevier, Oxford, **2007**, pp. 785 – 809.
[2] M. A. Méndez, R. Partovi-Nia, I. Hatay, B. Su, P. Ge, A. Olaya, N. Younan, M. Hojeij, H. H. Girault, *Phys. Chem. Chem. Phys.* **2010**, *12*, 15163 – 15171.
[3] a) S. Fukuzumi, K. Okamoto, C. P. Gros, R. Guilard, *J. Am. Chem. Soc.* **2004**, *126*, 10441 – 10449; b) A. Trojánek, V. Mareček, H. Jänchenová, Z. Samec, *Electrochem. Commun.* **2007**, *9*, 2185 – 2190; c) P. Peljo, L. Murtomäki, T. Kallio, H.-J. Xu, M. Meyer, C. P. Gros, J.-M. Barbe, H. H. Girault, K. Laasonen, K. Kontturi, *J. Am. Chem. Soc.* **2012**, *134*, 5974 – 5984.
[4] I. Hatay, B. Su, M. A. Méndez, C. Corminboeuf, T. Khoury, C. P. Gros, M. Bourdillon, M. Meyer, J.-M. Barbe, M. Ersoz, S. Záliš, Z. Samec, H. H. Girault, *J. Am. Chem. Soc.* **2010**, *132*, 13733 – 13741.
[5] A. Trojánek, J. Langmaier, Z. Samec, *Electrochem. Commun.* **2006**, *8*, 475 – 481.
[6] a) J. M. Campos-Martin, G. Blanco-Brieva, J. L. G. Fierro, *Angew. Chem.* **2006**, *118*, 7116 – 7139; *Angew. Chem. Int. Ed.* **2006**, *45*, 6962 – 6984; b) Q. Chen, *Chem. Eng. Process.* **2008**, *47*, 787 – 792; c) S. Lu, L. Wang, Y. Wang, Z. Mi, *Chem. Eng. Technol.* **2011**, *34*, 823 – 830; d) T. Nishimi, T. Kamachi, K. Kato, T. Kato, K. Yoshizawa, *Eur. J. Org. Chem.* **2011**, 4113 – 4120.
[7] J. R. T. J. Wass, E. Ahlberg, I. Panas, D. J. Schiffrin, *Phys. Chem. Chem. Phys.* **2006**, *8*, 4189 – 4199.
[8] S. Fukuzumi, Y. Yamada, K. D. Karlin, *Electrochim. Acta* **2012**, *82*, 493 – 511.
[9] a) A. K. Geim, K. S. Novoselov, *Nat. Mater.* **2007**, *6*, 183 – 191; b) A. K. Geim, *Science* **2009**, *324*, 1530 – 1534.
[10] M. D. Stoller, S. Park, Y. Zhu, J. An, R. S. Ruoff, *Nano Lett.* **2008**, *8*, 3498 – 3502.
[11] M. J. McAllister, J.-L. Li, D. H. Adamson, H. C. Schniepp, A. A. Abdala, J. Liu, M. Herrera-Alonso, D. L. Milius, R. Car, R. K. Prud'homme, I. A. Aksay, *Chem. Mater.* **2007**, *19*, 4396 – 4404.
[12] M. J. Allen, V. C. Tung, R. B. Kaner, *Chem. Rev.* **2010**, *110*, 132 – 145.
[13] D. Chen, H. Feng, J. Li, *Chem. Rev.* **2012**, *112*, 6027 – 6053.
[14] a) L. Tang, Y. Wang, Y. Li, H. Feng, J. Lu, J. Li, *Adv. Funct. Mater.* **2009**, *19*, 2782 – 2789; b) Y. Shao, J. Wang, M. Engelhard, C. Wang, Y. Lin, *J. Mater. Chem.* **2010**, *20*, 743 – 748; c) J. Wu, Y. Wang, D. Zhang, B. Hou, *J. Power Sources* **2011**, *196*, 1141 – 1144.
[15] G. Kalita, S. Sharma, K. Wakita, M. Umeno, Y. Hayashi, M. Tanemura, *Phys. Chem. Chem. Phys.* **2013**, *15*, 1271 – 1274.
[16] a) B. Su, R. P. Nia, F. Li, M. Hojeij, M. Prudent, C. Corminboeuf, Z. Samec, H. H. Girault, *Angew. Chem.* **2008**, *120*, 4753 – 4756; *Angew. Chem. Int. Ed.* **2008**, *47*, 4675 – 4678; b) R. Partovi-Nia, B. Su, F. Li, C. P. Gros, J.-M. Barbe, Z. Samec, H. H. Girault, *Chem. Eur. J.* **2009**, *15*, 2335 – 2340.
[17] J. J. Nieminen, I. Hatay, P. Ge, M. A. Mendez, L. Murtomaki, H. H. Girault, *Chem. Commun.* **2011**, *47*, 5548 – 5550.
[18] T. Wandlowski, V. Mareček, Z. Samec, *Electrochim. Acta* **1990**, *35*, 1173 – 1175.
[19] P. Ge, M. D. Scanlon, P. Peljo, X. Bian, H. Vubrel, A. O'Neill, J. N. Coleman, M. Cantoni, X. Hu, K. Kontturi, B. Liu, H. H. Girault, *Chem. Commun.* **2012**, *48*, 6484 – 6486.
[20] A. A. Karyakin, *Electroanalysis* **2001**, *13*, 813 – 819.
[21] R. M. Sellers, *Analyst* **1980**, *105*, 950 – 954.
[22] Y. Zhou, G. Zhang, J. Chen, G. e. Yuan, L. Xu, L. Liu, F. Yang, *Electrochem. Commun.* **2012**, *22*, 69 – 72.
[23] a) J. Xu, W. Huang, R. L. McCreery, *J. Electroanal. Chem.* **1996**, *410*, 235 – 242; b) H. H. Yang, R. L. McCreery, *J. Electrochem. Soc.* **2000**, *147*, 3420 – 3428.

Received: August 26, 2013
Revised: October 17, 2013
Published online on December 4, 2013